A Comparison of Methods for Determining Tropopause Height from VHF Radar Observations

W. B. SWEEZY AND E. R. WESTWATER

NOAA/ERL/Wave Propagation Laboratory, Boulder, CO 80303

(Manuscript received 26 June 1985, in final form 21 November 1985)

ABSTRACT

Four methods of estimating the height of the tropopause with VHF radar are compared and evaluated using data from a wind-profiling radar located at Platteville, Colorado, approximately 50 km north of Denver. An empirically derived method determines the tropopause height from the strength and persistence of the reflections. A second, theoretically based, method uses Fresnel scattering model estimates of the temperature gradient to determine the tropopause height. A third method identifies specular reflections associated with the tropopause by comparing vertical with oblique reflections. The final method combines the theoretically based method with a consensus set method for determining the most consistent estimates. The methods are compared by taking differences between the estimates and the tropopause heights determined from radiosonde data using the WMO definition of the tropopause. Each method is evaluated by calculating rms differences from the radiosonde determinations and by the number of differences that exceed an acceptable magnitude.

1. Introduction

The height of the tropopause is a useful parameter for a variety of applications including synoptic weather analyses and forecasting, aircraft flight planning and forecasting, and ozone concentration estimation (Reed and Danielson, 1959; Reiter et al., 1969). Our motivation for determining the tropopause height (at more optimum times and greater frequency than provided by radiosonde) is based on the desire to improve the retrieval of temperature profiles derived from remote radiometric measurements (Westwater and Grody, 1980). The largest statistical errors in both ground-based and satellite temperature retrievals are observed in the vicinity of the tropopause. Although the errors are significantly reduced by the combination of ground-based and satellite retrievals (Westwater et al., 1984), the maximum rms differences between combined retrievals and radiosonde soundings remain near the tropopause.

One of the most promising tools for remotely measuring the height of the tropopause utilizes the enhanced specular echoes reflecting from the tropopause observed with vertical pointing VHF radar (Gage and Green, 1978; Rötteger and Liu, 1978; Rötteger and Vincent, 1978). However, difficulties in determining the tropopause height from specular echoes arise from a variety of sources. For example, the data may be contaminated by radar returns from aircraft passing through the radar beam. Furthermore, there are the problems of distinguishing specular reflections from scatter due to isotropic or anisotropic turbulence, and of distinguishing the tropopause from other stable regions in the upper troposphere.

By examining profiles of vertical power return, one can usually subjectively locate the tropopause, but it is difficult, if not impossible, to adapt these subjective methods to automatic data processing. However, some investigators, including Zachs (Westwater et al., 1983) and Gage and Green (1982), have developed objective algorithms suitable for real-time computer calculation of the tropopause height. The Zachs algorithm was developed for computer use, and the Gage–Green algorithm was adapted for machine computation by Riddle et al. (1982). In this study, we compare the Zachs and Gage–Green methods with others, including a very promising variation of the Gage–Green algorithm.

2. Methods

a. Zachs

The Zachs algorithm is an empirically derived method that assigns the most persistent strong echo in a restricted height interval to the tropopause. The height interval is restricted by tropopause climatology. Examination of data showed that the temporal standard deviation of the signal-to-noise ratio (SNR) usually exhibited more pronounced peaks than the SNR itself. Therefore, Zachs developed algorithms based on the temporal standard deviation and its gradient above and below a peak echo. The persistence is measured by the autocorrelation of the SNR at the levels of the strong peaks.

The SNR standard deviation profile is calculated as

$$\sigma_h = \{\sum_{i=1}^{n} [S(t_i, h) - \bar{S}(h)]^2/(n-1)\}^{1/2}, \quad (1)$$

where

$$\bar{S}(h) = \sum_{i=1}^{n} [S(t_i, h)]/n,$$

n is the number of profiles spanned by the averaging time, and $S(t_i, h)$ is the SNR at time t_i and height h. The SNR is determined by the average of about 3×10^4 pulses. The standard deviation profiles are searched from the bottom to the top of the height interval to find peak values satisfying the following criteria: (i) a sharp increase (over one or two range gates) below the peak, (ii) a sharp decrease above the peak and (iii) the peak value exceeds a specified threshold. A scaled autocorrelation function

$$C(h) = \sum_{i=1}^{n-1} R(t_i, h)R(t_{i+1}, h) \quad (2)$$

is computed at each range gate satisfying the gradient and threshold criteria and at the range gate just below the peak, where

$$\left.\begin{aligned} R(t_i, h) &= S(t_i, h)/\sigma(t_i) \\ \sigma(t_i) &= \{\sum_{j=1}^{m} [S(t_i h_j) - \bar{S}(t_i)]^2/(m-1)\}^{1/2} \end{aligned}\right\}$$

is the spatial standard deviation over m range gates of the SNR profile at time t_i. The tropopause is assigned to the height with the largest correlation that exceeds an empirically determined threshold. The scaling by the spatial standard deviation attenuates the correlation for spurious peaks and enhances it for persistent peaks.

b. Gage–Green

The Gage–Green algorithm is based on the Fresnel scattering model described in detail by Gage et al. (1981). In the Fresnel scattering theory, the power reflection coefficient is proportional to the product of range resolution and the mean gradient of the generalized potential refractive index gradient, that is,

$$|\rho|^2 = [\Delta r f(\lambda)\bar{M}]^2,$$

where ρ is the power reflection coefficient, Δr is the range resolution, $f(\lambda)$ is an empirically determined function of wavelength, and M is the potential refractive index gradient. If we ignore the contribution of humidity, which is negligible near the tropopause, the potential refractive index gradient is given by

$$M = k\frac{p}{T}\frac{\partial \ln\theta}{\partial z} = k\frac{p}{T^2}\left(\Gamma + \frac{\partial T}{\partial z}\right),$$

where k is a constant, p is atmospheric pressure, T is absolute temperature, θ is potential temperature, and Γ is the dry adiabatic temperature lapse rate.

The range-corrected received power is related to the power reflection coefficient by the radar equation, so that

$$P_r = K_r^2\bar{M}^2,$$

where K_r is a system-dependent constant determined from the radar wavelength, the transmitted power, the effective area of the antenna, and an efficiency factor.

Assuming constant temperature in the stratosphere and an exponential decrease of pressure with height, Riddle et al. (1982) introduced a new parameter Q to facilitate automatic real-time computation of the tropopause height.

Let

$$p = p_0 \exp[-c(z - z_0)],$$

then

$$\ln P_r = 2\ln\left[K_c\frac{p_0}{T^2}\left(\Gamma + \frac{\partial T}{\partial z}\right)\right] - 2c(z - z_0),$$

where p_0 is pressure at the surface z_0, and K_c is a combination of k and K_r. The parameter Q is defined by

$$Q = \ln P_r + 2c(z - z_0), \quad (3)$$

and substitution for P_r yields

$$Q = 2\ln\left[K_c\frac{p_0}{T^2}\left(\Gamma + \frac{\partial T}{\partial z}\right)\right]. \quad (4)$$

From these equations we can compare a Q-profile derived from radar data using Eq. (3) with one derived from radiosonde (RAOB) data using Eq. (4). The hydrostatic constant c is determined from radiosonde pressure heights at 500 and 100 mb and the constant K_c is determined from the difference between the profiles. That is,

$$2\ln K_c = \ln P_r + 2c(z - z_0) - 2\ln\left[\frac{p_0}{T^2}\left(\Gamma + \frac{\partial T}{\partial z}\right)\right].$$

For each observed profile of received power a reference value

$$Q_0 = 2\ln\left(K_c\frac{p_0}{T^2}\Gamma\right)$$

can be calculated for the stratosphere with the assumption $\partial T/\partial z = 0$, by averaging over several range gates well above the tropopause. With these assumptions Eq. (4) becomes

$$Q = Q_0 + 2\left[\ln\left(\Gamma + \frac{\partial T}{\partial z}\right) - \ln\Gamma\right].$$

An example that illustrates the use of Eqs. (3) and (4) is shown in Fig. 1. Figure 1c shows Q calculated from the RAOB mandatory and significant level data, while 1b shows the RAOB-derived Q averaged over the

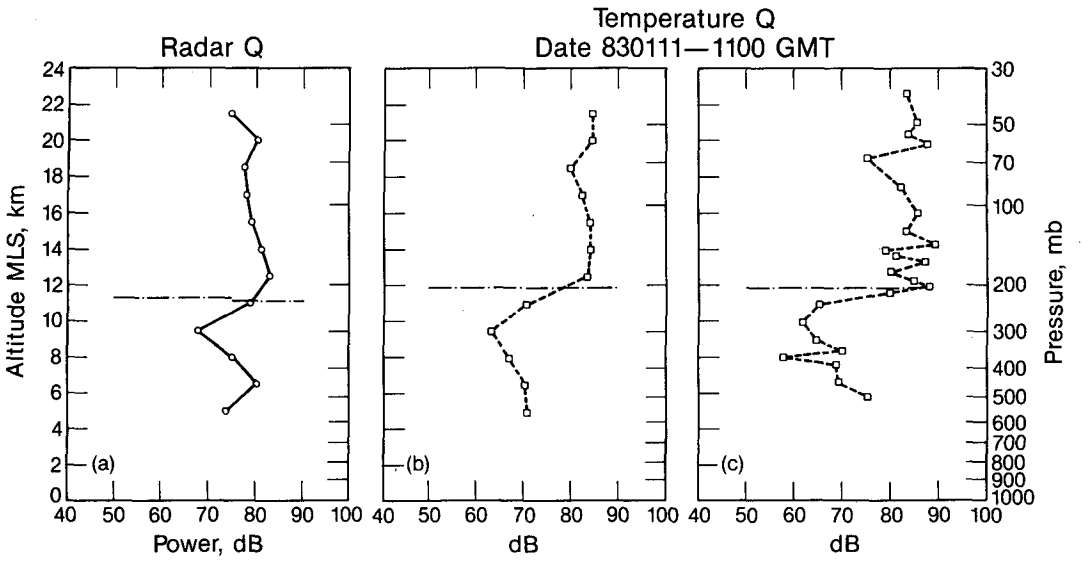

FIG. 1. (a) The range-corrected and pressure-normalized received power Q. The dashed lines are the Gage–Green estimates of the tropopause height. On the left is the consensus-set estimate, and on the right the average-power estimate. (b) and (c) The theoretical Q derived from the radiosonde temperature profile. In (b) the temperatures are interpolated to the range-gate heights, and in (c) the radiosonde mandatory and significant levels are used. Central differences are used to estimate the lapse rates. Dashed lines in (b) and (c) show the observed tropopause height according to the WMO definition.

radar range gate. The radar-derived Q, as shown in Fig. 1a shows good agreement with the averaged calculations. The significance of the dashed lines will be discussed in section 2d.

The value of Q at the tropopause with $\partial T/\partial z = -2$ K km^{-1} and $\Gamma = 9.8$ K km^{-1} is given by

$$Q_t = Q_0 - 0.20. \quad (5)$$

The height of the tropopause is determined by interpolating between range gates to find the height where Eq. (5) is satisfied.

Some recent modifications to the Gage–Green method by Gage et al. (1986b) are not included in this discussion. In the revised method, an exponential decrease with height of the backscattered power is taken into account (Gage et al., 1986a). These modifications produced an improved model for power profiles, but they appeared to have no effect on the tropopause height estimation.

c. *Specular reflection*

This simple technique compares backscattered power from vertical and off-vertical transmission for automatic machine identification of the tropopause. The enhanced specular echoes from the tropopause at vertical incidence are usually accompanied by diminished returns at oblique angles. The algorithm searches the vertical profile of range-corrected received power for peaks at heights where we expect to find the tropopause. The peak where the vertical power exceeds the average of the range-corrected power received from the two oblique beams by the largest amount is assigned to the tropopause, if the difference is greater than the specified minimum.

d. *Combined Gage–Green and consensus set*

The Zachs, Gage–Green, and specular reflection algorithms are all applied to a time-averaged power profile to determine the height of the tropopause. The main quality control is the selection of profiles to be averaged. With the consensus set algorithm a tropopause height is calculated for each individual profile using the Gage–Green method and a consensus set is selected from a series of individual profiles to determine the mean height of the tropopause for that time period.

The procedure for selecting the consensus set is adapted from Fischler and Bolles (1981). Each estimate of the tropopause height in the specified time span is compared with all of the others. The points that differ from the estimate by less than a specified maximum deviation $d_{\max}$ are counted. The consensus set is the set that contains the largest number of points within the deviation limits, provided that the number is greater than a specified minimum $N_{\min}$. Specifically, let L_i be the ith value of n tropopause height estimates. Then for each $j = 1, \cdots, n$, increment the count n_i if

$$|L_i - L_j| < d_{\max}.$$

Let $N = \max n_i$ for all i; if $N \geq N_{\min}$ then the consensus set is the N members of the subset counted. The tropopause height is determined by averaging the estimates in the consensus set.

An example of tropopause height determination by the Gage–Green method is shown in Fig. 1. The dashed line on the left in panel a is the consensus set estimate while the one on the right results from the average power estimate. The dashed lines in Figs. 1b and 1c show the tropopause height derived from radiosonde data.

3. Data selection and analysis

We gathered two years of radar and radiosonde data. Since these data were gathered to complement radiometric remote sensing activities, data were analyzed only when both ground-based Profiler and satellite-based NOAA 6, 7 or 8 soundings were available (Westwater et al., 1984). The sample was edited further by eliminating data for times when the vertical radar transmitter was malfunctioning and when the rawinsonde balloon flights did not extend to at least 2 km into the stratosphere. Radar power profiles were selected covering the time period from one hour before to one hour after the balloon launch. After selection and editing, 350 cases remained for analysis, covering a period from December 1981 to November 1983. The actual tropopause heights for comparison with the radar estimates were obtained from temperature profiles taken by radiosondes released at Stapleton International Airport in Denver by the National Weather Service. Radiosonde tropopause heights that we used in this paper were derived using the World Meteorological Organization (WMO) definition of the tropopause (Craig, 1965):

> At pressures of 500 mb or lower, the lowest level with respect to altitude h at which (a) the temperature lapse rate $-dT/dh$, decreases to 2°C km^{-1} or less, *and* (b) the average lapse rate from this level to any point within the next 2 km does not exceed 2°C km^{-1}.

The radar data were obtained from the (6-m wavelength) VHF radar located at the Platteville, Colorado Radar Facility approximately 50 km north of Denver at an elevation of 1523 m. The phased-array pulsed-Doppler radar transmits three beams—vertical, 15° north of vertical, and 15° east of vertical—and is primarily used to measure horizontal wind profiles. The radar is operated jointly by the Wave Propagation Laboratory and the Aeronomy Laboratory of NOAA; its operation is described in detail by Strauch et al. (1984). Each beam is usually sampled about every 5 min, with an averaging time of 78 s and a range-gate spacing of 1.5 km. The pulse width of 16 μs translates to a range resolution of 2.4 km. The range delay to the first gate varies from beam to beam to facilitate multiplexing. The range delay in the vertical is 1.85 km. Thirteen range gates extending to 21.37 km MSL are used in the analysis.

We selected the averaging time for Zachs, Gage–Green, and specular-reflection methods to be 1½ hours, beginning ½ hour before balloon release and ending 1 hour after, so that the balloon flight is approximately at 500 mb at the center of the averaging time. The averaging time was selected to optimize the Zachs algorithm that was developed using 20 min averages of one min samples (Westwater et al., 1983). The algorithm seems to perform best when the number of profiles averaged is between 18 and 22 (nearly equal to the number used in Zachs' original development). We did not attempt to optimize the averaging time for the other algorithms, but Riddle et al. (1982) achieved good results using 1-h averages.

Quality control for averaging the power profiles for the Gage–Green and specular methods eliminates spurious power peaks, presumably caused by aircraft, by deleting those that are more than 10 dB above the temporal median and eliminates weak signals by deleting those that are 10 dB or more below the median. Since we require equally spaced data for the Zachs method, it is not possible to delete data and the only quality control is provided by the scaled autocorrelation function, Eq. (2). Quality of the consensus set estimate is controlled by $d_{\max}$ (the maximum deviation), and by $N_{\min}$ (the minimum set-size parameter). The maximum deviation is set at 1 km, and $N_{\min}$ is one-third of the total sample size. In addition to a consensus mean for each sample, we record the variance and size of the consensus set. These parameters are used to improve the quality of the estimate, instead of manipulating $d_{\max}$ and $N_{\min}$. If the size of the consensus set is less than two-thirds of the sample size, we search for a secondary consensus that contains at least half of the remaining points and is at least 1.5 km from the primary consensus. Furthermore, for all methods, cases are deleted if the vertical power is less than the oblique power at all range gates above the second range gate (approximately 5 km MSL) or if the vertical power is 20 dB or more below the expected value. The tropopause height estimates are constrained to be between 6 and 17.5 km MSL, and to be greater than 8 km MSL in June through September.

For real-time implementation, the computation of the variance could be eliminated by tightening the restriction on the maximum allowable deviation $d_{\max}$, but it is necessary to search for secondary clusters unless $N_{\min}$ is made large enough to preclude their existence.

4. Results

A typical example is shown in Fig. 2 in which tropopause heights determined by the four methods are compared with the tropopause height determined from

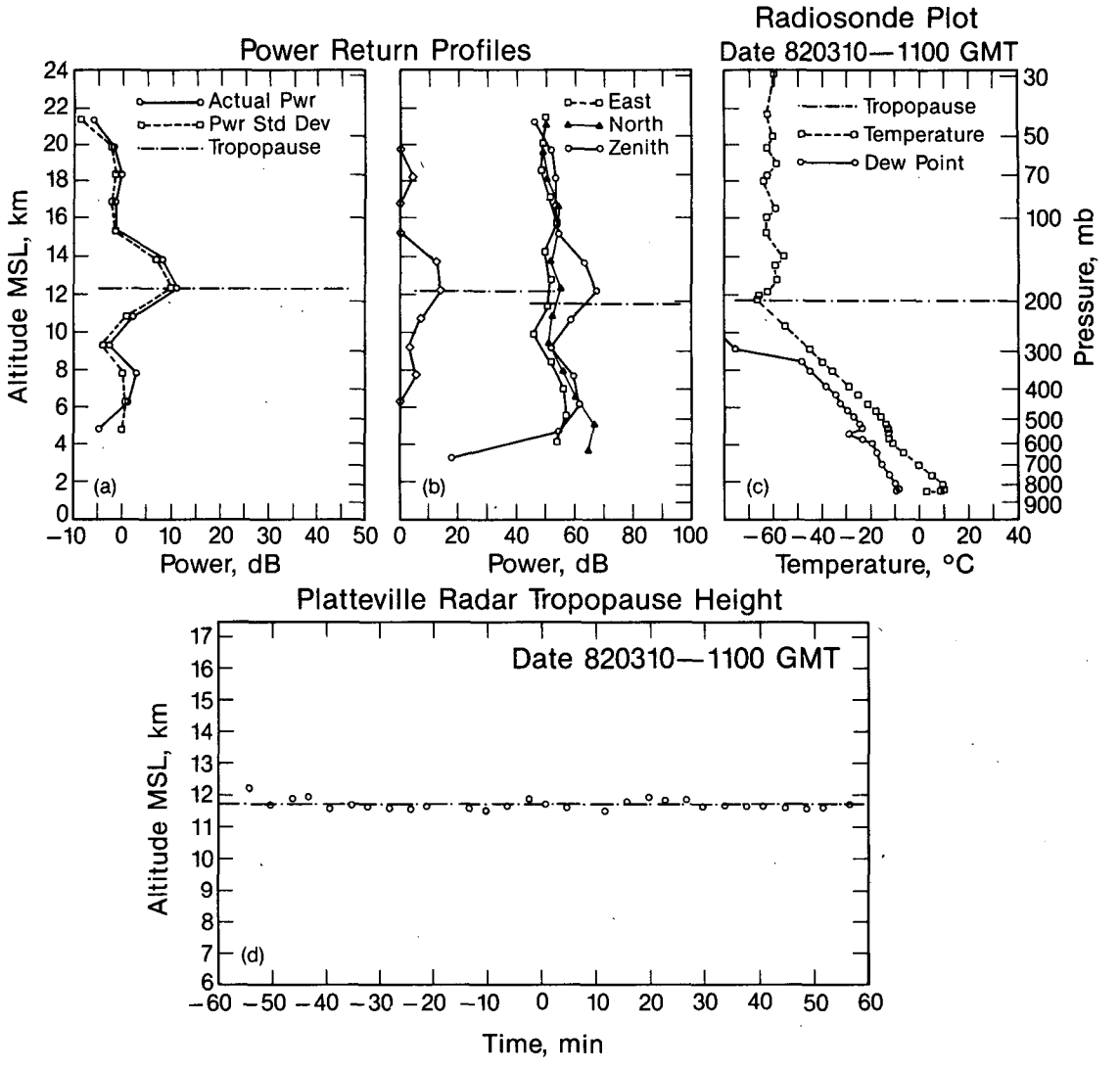

FIG. 2. Tropopause height estimates from the four methods, compared with the WMO defined tropopause. (a) The Zachs estimate; (b) the specular reflection estimate and difference between the vertical and oblique received power on the left and the Gage–Green estimate on the right; (c) the WMO definition; (d) the Gage–Green/consensus set estimate.

the radiosonde temperature sounding. Figure 2a shows the mean and standard deviation of the SNR used in the Zachs autocorrelation to estimate the tropopause height. Figure 2b shows the mean vertical power used for the Gage–Green algorithm, along with the mean oblique power from each direction, and the difference between the vertical and the average oblique power used for determining specular reflection. The power scale for Fig. 2b is different from Fig. 2a because the Zachs method normalizes the range correction to 12.9 km and all the other methods normalize to 1 km. Figure 2c shows the radiosonde temperature and dewpoint profiles with a well defined tropopause. Figure 2d shows the individual estimates and the consensus average estimate of the tropopause height.

The results are equally good for all methods for the case shown in Fig. 2. However, over the entire dataset this was not always true. Table 1 presents statistics representing the entire two-year period; there are isolated examples when each method outperforms all of the others, but it is clear that the Gage–Green method is a superior estimator that is greatly enhanced by fine tuning with the consensus set method. Table 1 lists the methods in order of improvement as determined by decreasing rms differences and a decreasing number of outliers (any estimate that differs from the radiosonde tropopause by more than the range gate spacing is considered an outlier). The entries for the consensus set method are computed using one-third of the sample size for $N_{\min}$ and 1 km for $d_{\max}$.

TABLE 1. Methods for determining tropopause height.

Method	Number of estimates	Bias (km)	Rms difference (km)	Maximum absolute difference (km)	Number of absolute differences greater than 1.5 km
Zachs	332	−0.098	5.409	7.780	119
Specular reflection	262	0.503	2.131	8.004	87
Gage–Green	338	−0.403	1.587	6.626	59
Consensus set	337	−0.352	1.483	7.852	47
with variance < 0.4	321	−0.338	1.457	7.852	38
with $N \geq$ ½ total	305	−0.339	1.117	7.852	28
without secondary consensus	283	−0.229	1.028	6.924	25
combined	264	−0.277	0.848	5.062	15
Ideal (outliers removed)	249	−0.207	0.538	1.421	0

The entries following the consensus set entry are for those cases in which (i) the variance of the consensus is less than 0.4 (km^2), (ii) the size of the consensus set is at least one-half the sample size, (iii) there is no secondary consensus, and (iv) the first three are applied simultaneously. In cases where a secondary consensus exists, we attempted to use climatological and persistence criteria to select a tropopause height from the primary or secondary consensus. These criteria misidentified the tropopause in too many cases to be useful. In several cases the existence of a secondary consensus is due to a poorly defined tropopause or to a weak signal. Efforts to utilize the secondary consensus sets to improve the tropopause height estimates failed to yield consistent results, but Table 1 shows that the quality is greatly improved if these cases are eliminated. The "ideal" entries are the "combined" with the outliers eliminated. By including the more restrictive parameters of the combined conditions we eliminate 32 outliers by deleting only 73 cases.

If we examine a few cases with apparent outlying estimates we see that these may be better than indicated. Figure 3 shows four cases in which the radar estimates (Gage–Green and Gage–Green/consensus) may be the "correct" tropopause height. In Figs. 3a–c, the lapse rate from the radar tropopause to the WMO tropopause is less than 2.5 K km^{-1}, exceeding the WMO requirement by less than 0.5 K km^{-1}. Furthermore in Figs. 3b and 3c the lapse rate is less than 2 K km^{-1} for about 1.8 km above the radar estimate of tropopause and is only 200 meters short of the WMO thickness requirement. The case in Fig. 3d has a radar estimate that is higher than the WMO tropopause, but is similar in structure to the other cases. In each case there is a very thin layer at the WMO tropopause with a lapse rate substantially different from the adjacent layers.

Figure 4 shows the worst case, that is, the one with the greatest absolute difference between the radar estimates and the WMO tropopause. Each method selected a tropopause near 11 km. The specular reflection and Gage–Green estimates are shown in Fig. 4a, and the consensus estimate is shown in Fig. 4c. The Zachs estimate is not shown, but it is identical to the specular reflection estimate. Regardless of the actual location of the tropopause in this case, the important question for our purpose is: Would the information that there is a substantial stable layer near 11 km enhance (at least, not degrade) the radiometric temperature retrieval? The answer to that question is the subject of another study by the authors, but we can conjecture at this point that such information would be useful. In addition, as pointed out by an anonymous reviewer, the distinction between the troposphere and stratosphere cannot always be determined on the basis of a sounding at a single location. This is especially true during frontal passages. However, it is clear that monitoring of stable layers, even if they do not define the tropopause, will provide meteorologists with useful information.

Nearly all of the outlying cases were similar to the five discussed and the same question and conjecture posed for the case in Fig. 4 would apply to them.

5. Summary and discussion

The comparisons show that in the present state of development the Zachs and specular reflection methods are not applicable to real-time estimation of the tropopause, because of an excessive number of estimates with large errors. The Gage–Green method appears to be a better estimate than either Zachs or specular reflection. Furthermore, consensus sampling eliminates most of the erroneous Gage–Green estimates, but does not apply to the Zachs algorithm.

The method that uses the most stringent quality controls achieved a 78% yield with a 6% false identification rate. For this high quality dataset, the rms difference between radiosonde-measured and radar-inferred tropopause height was 0.85 km. An examination of the 15 cases of false identification showed that most were situations in which the tropopause was not well defined; e.g., either a "double" tropopause or a transitional meteorological situation was occurring.

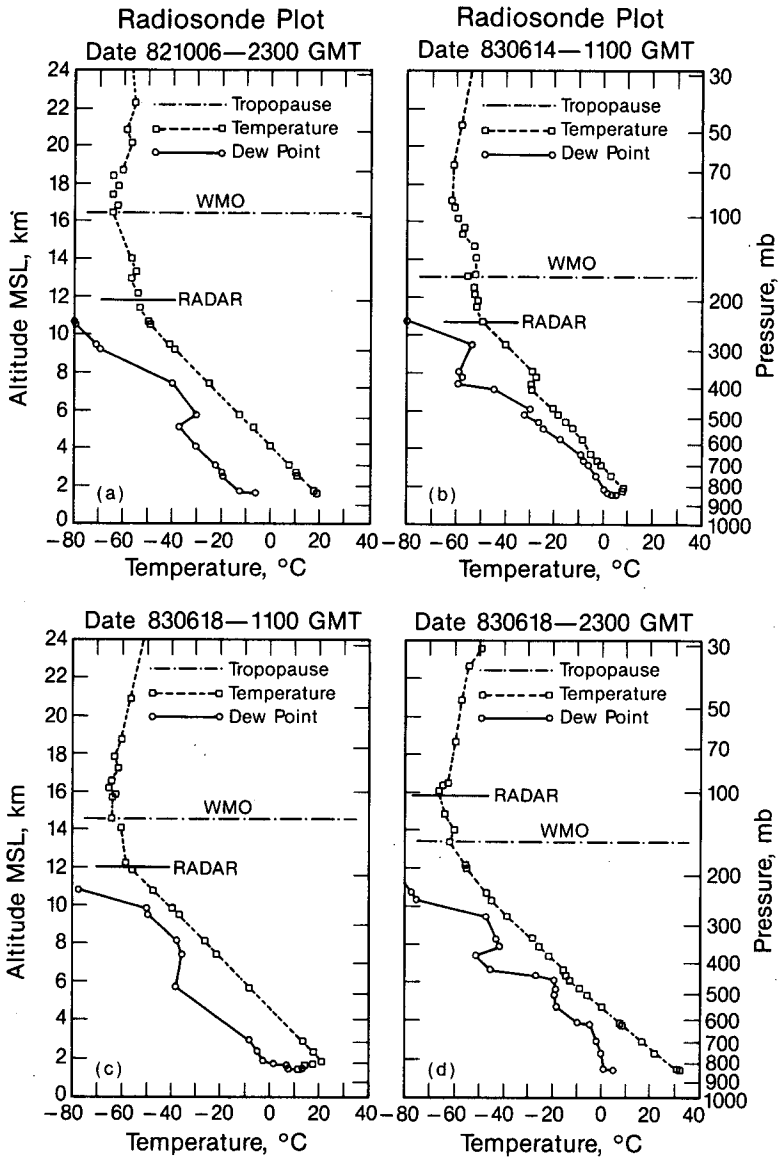

FIG. 3. Cases with multiple stable layers in the region of the atmosphere where the tropopause is expected to be located in which the radar estimate differs significantly from the WMO definition.

Examining the time series of the 5-min samples of tropopause height showed several distinct and potentially meaningful patterns. If the tropopause was sharply defined and stable in time, the variance of the time series was small. Conversely, if there was a relatively smooth change in lapse rate at the tropopause, the corresponding variance was large, but centered about a mean value. When there were two (or more) stable layers that were largely separated, the data points would sometimes jump randomly from one level to the other. Finally, on several occasions, periodic oscillations in the data could be seen. These oscillations were quite suggestive of atmospheric wave behavior, such as gravity waves. Temporal modulation of the temperature structure at tropopause altitudes by gravity waves could also lead to differences between radar and radiosonde. This modulation could cause the tropopause height to shift into adjacent radar range gates, and, in a worst case situation, could lead to a large discrepancy.

Finally, as pointed out by an anonymous reviewer, the transition from troposphere to stratosphere can occur within a broad transition region, and that in such cases an *arbitrary* definition must be employed to de-

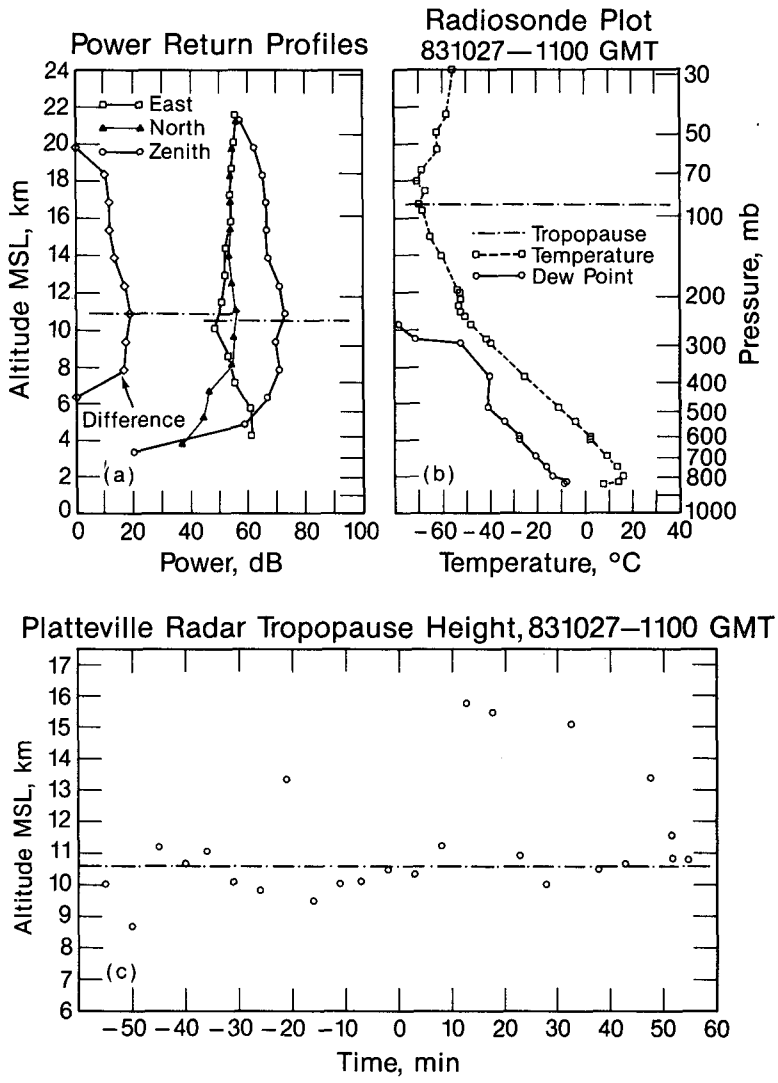

FIG. 4. The worst case. Every method, (a) Zachs and specular-reflection on the left and Gage–Green on the right and (c) Gage–Green/consensus-set, identified a stable layer that does not quite satisfy (b) the WMO definition.

fine a point called the tropopause. We agree with this comment and suggest that both the temporal and vertical spatial behavior of reflectivity profiles can provide significant meteorological information. It is really only a first cut in quantifying this information to derive a single parameter, i.e., the tropopause height, from the radar data. In a similar vein, the use of tropopause height to improve radiometrically sensed temperature profiles is only a crude step in combining active and passive information. In all likelihood, an optimum profile retrieval algorithm would use reflectivity information from all range gates, as well as radar-derived winds.

Acknowledgments. We are grateful for the cooperation and assistance of C. Gordon Little, Dave Hogg, Ken Gage, and Tony Riddle in many fruitful discussions. We thank Kathy Sweeney for her assistance in organizing and editing the data and for providing the computer graphics. The comments provided by anonymous reviewers were also helpful.

REFERENCES

Craig, R. A., 1965: *The Upper Atmosphere: Meteorology and Physics.* Academic Press, 23–25.

Fischler, M. A., and R. C. Bolles, 1981: Random sample consensus: A paradigm for model fitting with application to image analysis and automated cartography. *Commun. ACM,* **24,** 381–395.

Gage, K. S., and J. L. Green, 1978: Evidence for specular reflection from monostatic VHF radar observations of the stratosphere. *Radio Sci.,* **13,** 991–1001.

——, and ——, 1982: An objective method for determination of tropopause height from VHF radar observations. *J. Appl. Meteor.*, **21,** 1159–1163.

——, B. B. Balsley and J. L.Green, 1981: A Fresnel scattering model for the specular echoes observed by VHF radar. *Radio Sci.*, **16,** 1447–1453.

——, W. L. Ecklund and B. B. Balsley, 1986a: A modified Fresnel scattering model for the parameterization of Fresnel returns. *Radio Sci.*, **20,** 1493–1501.

——, ——, A. C. Riddle and B. B. Balsley, 1986b: Objective tropopause height determination using VHF radar. *J. Atmos. Ocean Technol.*, **3,** 248–254.

Reed, R. J., and E. F. Danielsen, 1959; Fronts in the vicinity of the tropopause. *Arch. Meteor. Geophys. Bioklim,* **A11,** 1–11.

Reiter, E. R., M. E. Glasser and J. D. Mahlman, 1969: The role of the tropopause in the stratosphere—troposphere exchange processes. *Rev. Geophys. Space Phys.*, **13,** 459–473.

Riddle, A. C., K. S. Gage and B. B. Balsley, 1982: Title, *Preprints, 21st Conf. Radar Meteorology,* Edmonton, Amer. Meteor. Soc., 153–157.

Rötteger, J., and C. H. Liu, 1978: Partial reflection and scattering of VHF radar signals from the clear atmosphere. *Geophys. Res. Lett.*, **5,** 357–360.

——, and R. A. Vincent, 1978: VHF radar studies of tropospheric velocities and irregularities using spaced antenna techniques. *Geophys. Res. Lett.*, **5,** 917–920.

Strauch, R. G., D. A. Merritt, K. P. Moran, K. B. Earnshaw and D. van de Kamp, 1984: The Colorado wind-profiling network. *J. Atmos. Oceanic Technol.*, **1,** 37–49.

Westwater, E. R., and N. C. Grody, 1980: Combined surface and satellite based microwave temperature profile retrieval. *J. Appl. Meteor.*, **19,** 1438–1444.

——, M. T. Decker, A. Zachs and K. S. Gage, 1983: Ground-based remote sensing of temperature profiles by a combination of microwave radiometry and radar. *J. Climate Appl. Meteor.*, **22,** 126–133.

——, W. B. Sweezy, L. M. McMillin and C. Dean, 1984: Determination of atmospheric temperature profiles from a statistical combination of ground-based profiler and operation NOAA 6/7 satellite retrievals. *J. Climate Appl. Meteor.*, **23,** 689–703.